Journal of Biomolecular NMR, 7 (1996) 163–168
ESCOM

J-Bio NMR 336

Measurement of $^{13}C^{\alpha}$-^{13}CO cross-relaxation rates in ^{15}N-/^{13}C-labelled proteins

Florence Cordier, Bernhard Brutscher and Dominique Marion*

Institut de Biologie Structurale-Jean Pierre Ebel, C.E.A.-C.N.R.S., 41 Avenue des Martyrs, F-38027 Grenoble Cédex, France

Received 22 November 1995
Accepted 23 January 1996

Keywords: ^{13}C-^{13}C cross relaxation; Nuclear Overhauser effect; Internal motions; Dipolar relaxation; Spectral density function; Cytochrome

Summary

Internal motions play an important role in the biological function of proteins and NMR relaxation studies may characterize them over a wide range of frequencies. An experimental pulse scheme is proposed for the measurement of the ^{13}CO-$^{13}C^{\alpha}$ cross-relaxation rate. For sensitivity reasons, this measurement is performed in an indirect manner through several coherence transfer steps, which should thus be calibrated independently. Contributions of other relaxation pathways can be eliminated by the determination of the initial slope of the buildup curve. The cross-relaxation rates have been determined on a ^{15}N-/^{13}C-labelled 116-residue protein and the significant variations along the sequence have been interpreted as evidence of an increased amount of fast local motion.

In solution, proteins undergo a wide variety of motions, ranging from atomic fluctuations and bond oscillations to local or global unfolding processes (Brooks et al., 1988). Intramolecular fluctuations can be characterized either by theoretical (e.g. molecular dynamics simulations up to the nanosecond time scale (Chandrasekhar et al., 1992; Van Gunsteren, 1993; Smith et al., 1995)) or experimental (e.g. NMR relaxation measurements (Kay et al., 1989)) techniques. Experimental evidence, however, suggests that slower motions are present, for example differences in cross-peak intensities in homo- and heteronuclear NMR experiments.

In principle, the measurement of NMR relaxation rates gives access to molecular motions, provided that the mechanisms and the partner distances are known. Therefore, attention has been focused so far on the backbone ^{15}N (Peng and Wagner, 1992a) or $^{13}C^{\alpha}$ nuclei (Yamazaki et al., 1994; Engelke and Rüterjans, 1995). Relaxation of these spins is principally controlled by the chemical shift anisotropy (CSA) of ^{15}N (or ^{13}C) and the dipole–dipole (DD) interaction with the directly attached proton. Except for rotating frame spin–lattice relaxation ($T_{1\rho}$) experiments, which detect dynamics occurring in the microsecond time range (Kopple et al., 1988; Ikuta and Wang, 1990), NMR relaxation experiments cannot monitor internal motions that are slower than the overall tumbling (Lipari and Szabo, 1982a).

The measured relaxation rates are then interpreted in two ways: either in terms of a fast internal motion superposed on a slower overall tumbling (the spatial restriction of the NH (or C^{α}-H) vector is then characterized by an order parameter S^2 (Lipari and Szabo, 1982a,b)), or in a more general approach (Peng and Wagner, 1992a,b), simply as frequency components of the spectral density function $J(\omega)$. In the case of eglin c, it has been shown (Peng and Wagner, 1992a) that the spectral density functions at lower frequencies ($J(0)$ and $J(\omega_N)$) are much larger and less uniform (and possibly more interesting) than the higher frequency terms ($J(\omega_H + \omega_N)$, $J(\omega_H)$ and $J(\omega_H - \omega_N)$). If the Lipari–Szabo approach is used, a similar pattern is observed on the order parameter S^2. Generally, the order parameter found for structured NHs lies between 0.8 and 0.85, and lower S^2 values are then interpreted as evidence of the presence of further internal motion.

Relaxation probes used so far have all involved a proton, and one may wonder whether vectors between heavy atoms of the backbone (such as CO, C^{α} or N) also dis-

*To whom correspondence should be addressed.

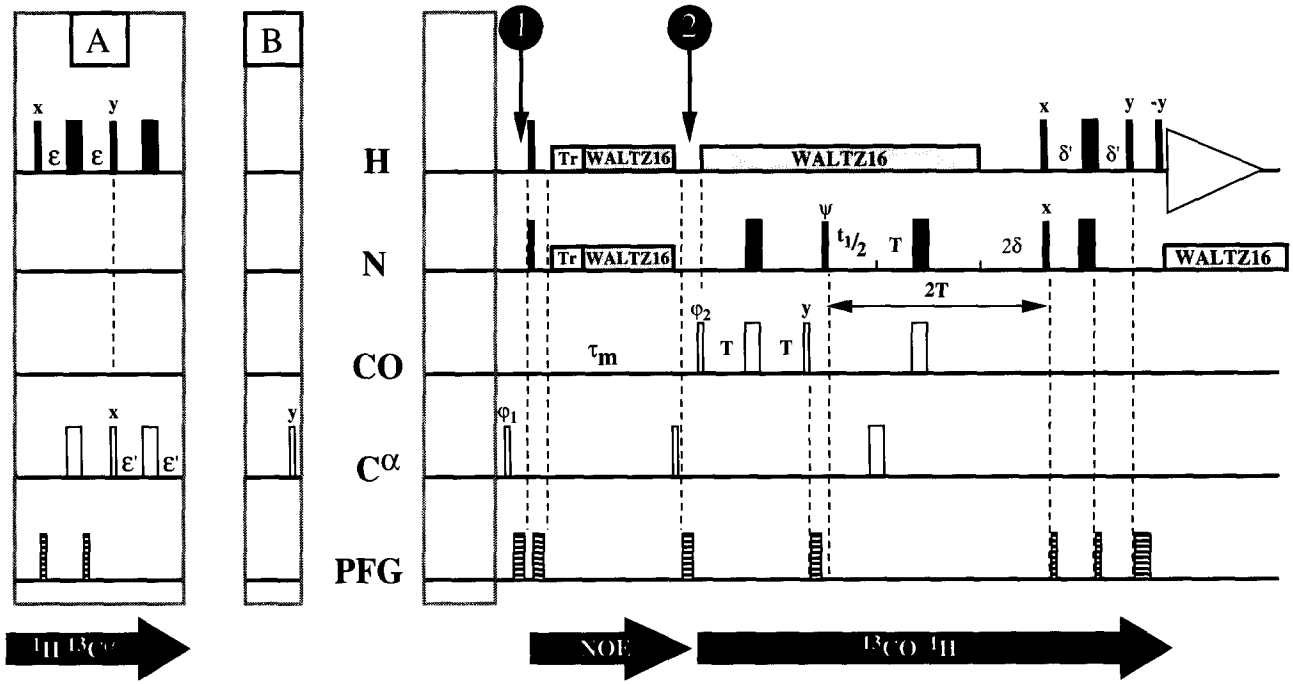

Fig. 1. Pulse sequence used for the measurement of $^{13}C^{\alpha}$-^{13}CO cross-relaxation rates. The first part of the sequence can be replaced either by insert A (refocused INEPT transfer) or by insert B (single 90° pulse on $^{13}C^{\alpha}$). Narrow and wide pulses correspond to 90° and 180° flip angles, respectively (applied along the x-axis unless indicated otherwise). All ^{1}H and ^{15}N pulses are applied at high power level, whereas square-shaped pulses are used on the ^{13}C channel, with zero excitation on the CO or C^{α} frequency. Compared to standard triple-resonance experiments, this calibration must meet much higher standards to avoid residual CO_z magnetization. The saturation of the ^{1}H and ^{15}N is achieved in the following manner: a 90° pulse, a pulse field gradient, four trim pulses of 2 ms duration (with respective phases x, y, –x, –y), and composite WALTZ decoupling. Coherence transfer pathway selection is achieved using pulsed field gradients (100–800 μs, ≈ 20 G/cm), as indicated in the sequence, and the phase cycling is as follows: $\varphi_1 = y,-y$; $\varphi_2 = 2(x),2(-x)$; $\psi = 4(y),4(-y)$; $\varphi_{rec} = (x,-x,-x,x,-x,x,x,-x)$. Two-dimensional spectra on *Rb. capsulatus* cytochrome c_2 were recorded using the following carrier frequencies and spectral widths: $^{1}H = 4.725$ ppm, 7246 Hz; $^{15}N = 121.8$ ppm, 1824 Hz; $^{13}C^{\alpha} = 58.2$ ppm, and $^{13}CO = 174.8$ ppm. The transfer delays were set to: $\varepsilon = 1.3$ ms, $\varepsilon' = 1.1$ ms (as a compromise for CH and CH_2), $T = 14$ ms, $2\delta = 5.4$ ms and $\delta' = 2.25$ ms. The spectral resolution in the ^{15}N dimension was doubled using mirror image linear prediction (Zhu and Bax, 1990) prior to Fourier transformation. Quadrature detection was achieved in t_1 by incrementing the phase ψ according to the States-TPPI method (Marion et al., 1989). Possible thermal drift due to the ^{1}H and ^{15}N saturation was compensated by off-resonance irradiation during the relaxation delay.

play low order parameters, i.e., large amounts of fast motion. It is obvious that a vector such as C^{α}-CO is sterically more hindered than an NH vector and molecular dynamics simulations carried out in our laboratory (M.J. Blackledge, IBS, Grenoble, France, personal communication) have shown that S^2 values associated with C^{α}-CO vectors are on average larger than those associated with NH (0.95 instead of 0.85).

We have chosen to investigate the cross-relaxation rate ($\sigma_{CO C^{\alpha}}$) of a $^{13}C^{\alpha}$-^{13}CO spin system in order to exploit the fact that the two types of spin can still be manipulated in an independent manner using semiselective pulses, but map the spectral density function at very low frequency (≈ 20 kHz). When true heteronuclear spin systems such as NH are used, the spectral density function at low frequency (J(0)) is inferred from transverse relaxation rates, to which chemical exchange may contribute. With a homonuclear spin system such as C^{α}-CO, $J(\omega_{C^{\alpha}} - \omega_{CO})$ provides a reasonable estimate of J(0) (or of S^2) via longitudinal relaxation times.

In the well-known case of ^{1}H-^{1}H NOE, the cross-relaxation rates are commonly measured either in the presence of a saturating field (truncated driven NOE (Wagner and Wüthrich, 1979)) or after selective inversion of one of the spins (transient NOE). These two methods can also be implemented for the measurement of $^{13}C^{\alpha}$-^{13}CO cross-relaxation rates. In an accompanying paper, Zeng et al. (1996) determine the $^{13}C^{\alpha}$-^{13}CO steady-state NOE and convert it into cross-relaxation rates using an independent measure of the ^{13}CO longitudinal relaxation (T_1). In this communication, we present a method for direct measurement of the $^{13}C^{\alpha}$-^{13}CO cross-relaxation rate as the initial slope of a buildup curve. This rate has to be normalized with respect to a calibration experiment, as for instance in the case of NOESY cross peaks with respect to the diagonal peak. The approach will be demonstrated on a 2 mM uniformly ^{15}N-/^{13}C-labelled sample of *Rhodobacter capsulatus* ferrocytochrome c_2, a 116-residue protein acting as a soluble electron transporter between membrane-bound redox centers.

For reasons of sensitivity and spectral resolution, the $^{13}C^{\alpha}$-^{13}CO NOEs are detected indirectly in a triple-resonance experiment. Two different but symmetrical coherence transfer pathways can be devised:

$$[^1H^{\alpha} \rightarrow] \, ^{13}C^{\alpha} \xrightarrow{NOE} {}^{13}CO \rightarrow {}^{15}N \rightarrow {}^{1}H^{N} \quad (1a)$$

$$[^1H^{N} \rightarrow {}^{15}N \rightarrow] \, ^{13}CO \xrightarrow{NOE} {}^{13}C^{\alpha} \rightarrow {}^{1}H^{\alpha} \quad (1b)$$

In both schemes, the magnetization can originate directly from either ^{13}C or ^{1}H via a coherence transfer scheme, indicated in brackets. Since the direct observation of H^{α} under a large water signal in the latter scheme (1b) is less convenient and the spectral resolution of H^{N} is favorable compared to that of H^{α}, the first scheme (1a) has been implemented, as shown in Fig. 1. In insert A of Fig. 1, the C^{α} spins are polarized using a refocused INEPT transfer, while a single 90° pulse is used in insert B. The additional INEPT step increases the sensitivity (by a theoretical factor γ_H/γ_C if relaxation during the transfer step is neglected), but requires an additional calibration experiment (see discussion below). During the mixing time τ_m (between points ❶ and ❷), the C^{α} longitudinal magnetization is allowed to exchange magnetization with CO by DD interaction. Finally, the z-magnetization of the CO is transferred to the amide proton in a way similar to the constant-time HNCO experiment proposed by Grzesiek and Bax (1992).

For protein applications, the need for adequate resolution dictates that at least two-dimensional correlation spectra are recorded. Labelling of the C^{α} nucleus would unambiguously identify one of the two interaction partners, but this nucleus exhibits unfavourable transverse relaxation and cannot be labelled here in a constant time fashion (Bax et al., 1979). Consequently, this leaves us free to label either ^{13}CO or ^{15}N (or both in the case of a 3D experiment) using a constant-time method during a $2T = (2 \times {}^{1}J_{NCO})^{-1}$ transfer period, thus obtaining comparable spectral and digital resolution for either nucleus. For convenience, the ^{15}N spins have been labelled to obtain a ^{1}H-^{15}N HSQC-like display. However, due to a lack of frequency labelling prior to τ_m, attention must be paid to strictly control the coherence transfer pathways before and after the mixing. The C^{α} pulses were carefully calibrated in order to minimize the excitation of the CO and pulsed field gradients, and phase cycling (as indicated in the legend of Fig. 1) was used for coherence pathway selection. In addition, a C^{α} 90° pulse, followed by a pulsed field gradient, is added at the end of τ_m to eliminate remaining C^{α} magnetization, which could be accidentally transferred to an amide proton due to the similar magnitude of the $^{1}J_{NCO}$ and $^{1}J_{NC^{\alpha}}$ scalar couplings and imperfections of the selective ^{13}C pulses.

If we consider the evolution of the CO magnetization during the NOE mixing period, it is clear that the only spins which can exchange magnetization with C^{α} are the CO and the C^{β}. Cross relaxation with ^{1}H and ^{15}N spins is eliminated by their saturation throughout τ_m. Because the C^{β} chemical shift range partially overlaps with that of C^{α}, selective saturation of the C^{β} is not achievable during the mixing time τ_m. In addition, the C^{α} pulses (before point ❶) will also affect to some extent the C^{β} spins. This results in a cross-relaxation term between the two ^{13}C spins, which yields a small change of the C^{α} magnetization, but will not significantly disturb the C^{α}-CO transfer of interest. On the other hand, direct cross relaxation between C^{β} and CO can be neglected because of their large separation (> 2.5 Å).

If only dipolar relaxation is taken into account, no transfer occurs between the longitudinal magnetization C_z^{α} (or CO_z) and longitudinal z-order $C_z^{\alpha}CO_z$, because these coherences do not share the same symmetry with respect to spin inversion (Werbelow and Grant, 1977). However, as demonstrated by Goldman (1984), cross correlation between CSA and the dipolar relaxation mechanism allows a two-step indirect transfer $C_z^{\alpha} \rightarrow C_z^{\alpha}CO_z \rightarrow$

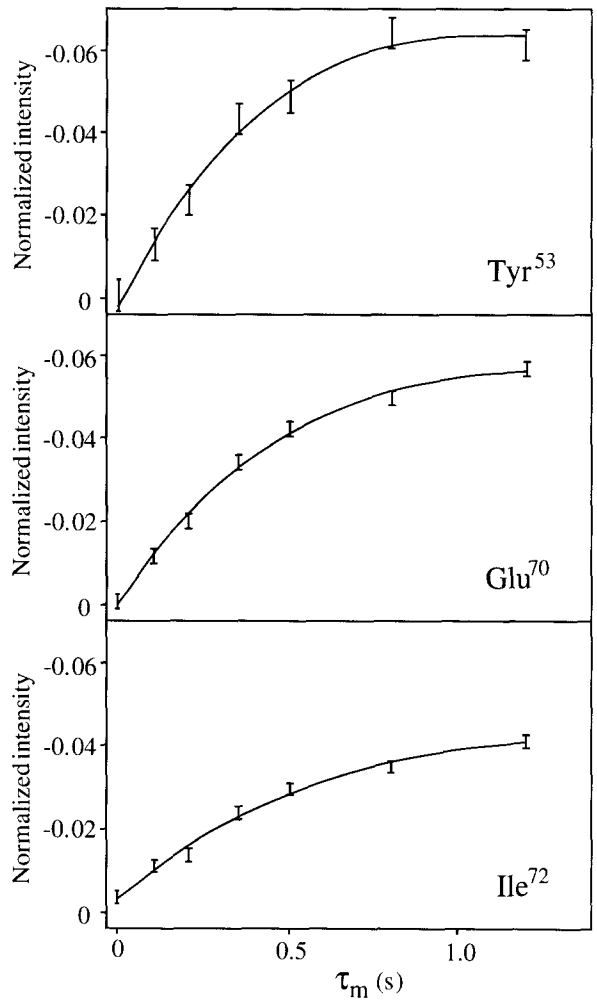

Fig. 2. Normalized buildup curves of $^{13}C^{\alpha}$-^{13}CO NOE for residues Tyr^{53}, Glu^{70} and Ile^{72} of *Rb. capsulatus* ferrocytochrome c_2. The buildup curve has been sampled at seven different mixing times (0, 100, 200, 350, 500, 800 and 1200 ms). The cross-peak intensities (vertical scale) have been normalized using calibration experiments, as indicated in the text. The error bars reflect the S/N ratios of the 2D spectra. The experimental points are fit with four parameters according to Eq. 2, $\sigma_{CO^{\alpha}}$, $\rho_{C^{\alpha}}^{eff} - \rho_{CO}$, ρ_{CO} and an offset parameter.

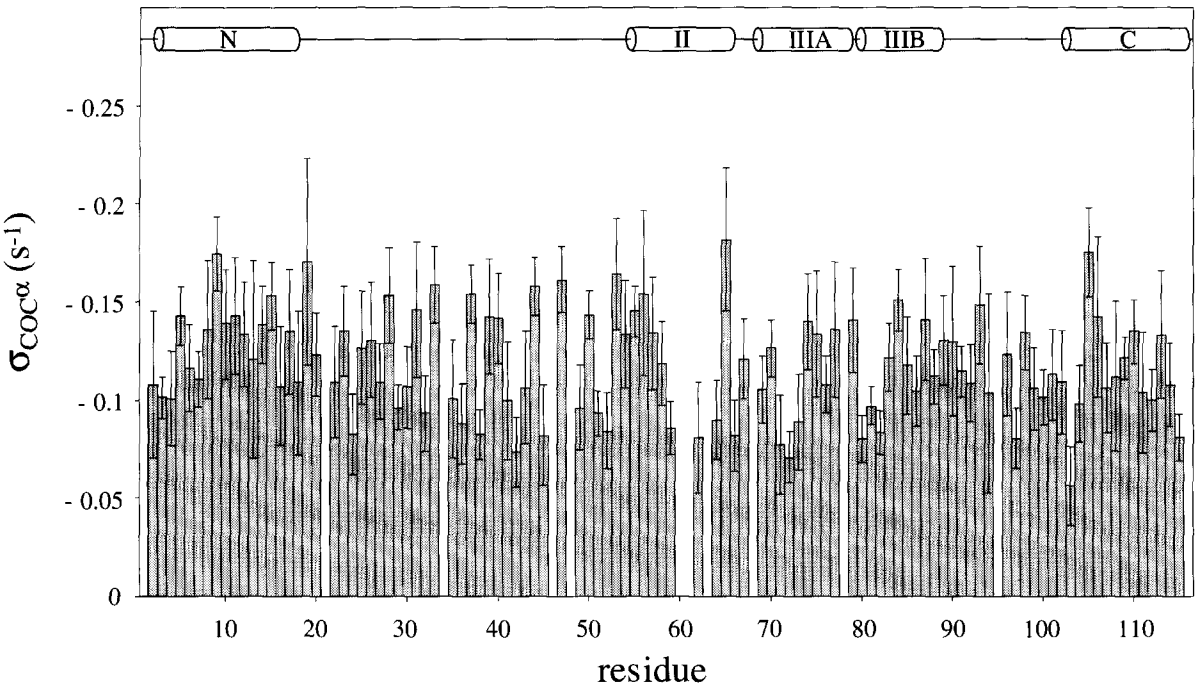

Fig. 3. Histogram of the measured $\sigma_{C^\alpha CO}$ values as a function of the amino acid sequence of *Rb. capsulatus* ferrocytochrome c_2. Note the negative sign of $\sigma_{C^\alpha CO}$. Statistical error bars have been calculated for each residue, taking into account the error in the curve fit as well as in the cross-peak intensities of the two calibration experiments. A fit of the experimental curves with only three parameters (without the offset) narrows the error bars by a factor of 2, but does not significantly modify $\sigma_{C^\alpha CO}$. The regular secondary structural elements of *Rb. capsulatus* cytochrome c_2 are shown at the top.

CO_z. Numerical simulations show that the rate of the first step is about 10 times smaller than the cross-relaxation rate σ_{COC^α}.

Therefore, as a useful approximation, one can discard the $C_z^\alpha CO_z$ coherence in the following discussion and analyse a simple (as if non-J-coupled) two-spin system (CO-C^α) with an effective autorelaxation rate $\rho_{C^\alpha}^{eff} \approx \rho_{C^\alpha} + \sigma_{C^\alpha C^\beta}$. Since for proteins $\sigma_{COC^\alpha} \ll \rho_{CO}$, the cross-relaxation equation for a two-spin system can be simplified to:

$$CO_z(\tau_m) \approx C_z^{\alpha^{eq}} \times \frac{2\,\sigma_{COC^\alpha}}{\rho_{C^\alpha}^{eff} - \rho_{CO}} \times \exp(-\rho_{CO}\,\tau_m) \times \left[1 - \exp(-(\rho_{C^\alpha}^{eff} - \rho_{CO})\tau_m)\right] \quad (2)$$

and in the initial slope approximation the CO magnetization is given by:

$$\left.\frac{d}{dt} CO_z(t)\right|_{t=0} = 2\,\sigma_{COC^\alpha} C_z^{\alpha^{eq}} \quad (3)$$

In our experiments, the $C^\alpha \rightarrow$ CO NOE is measured in an indirect manner. We define two transfer coefficients, which have to be added as additional factors in Eqs. 2 and 3: (i) $F_{H\rightarrow C^\alpha}$ when a $^1H \rightarrow {}^{13}C$ INEPT is used at the beginning instead of a simple 90° excitation pulse; and (ii) $F_{CO\rightarrow H}$ for the final CO-NH transfer step. On account of the differences in relaxation and J-coupling, the values of these coefficients depend on the individual residue and have to be determined by calibration experiments.

In practice, the $F_{H\rightarrow C^\alpha}$ coefficient can be measured by comparing the signal intensity of two experiments, recorded respectively with inserts A (INEPT) and B (90°) of Fig. 1 at a fixed mixing time τ_m. A compromise for the INEPT delay was found in order to correctly excite all C^α, including the glycines (CH_2) (Sørensen and Ernst, 1983). High precision on $F_{H\rightarrow C^\alpha}$ is obtained by choosing a mixing time close to the maximum of the NOE buildup (higher S/N). Instead of the theoretical value of 4 ($\approx \gamma_H/\gamma_C$), we found an enhancement of $F_{H\rightarrow C^\alpha}$ varying from 1.5 to 3.0 for *Rhodobacter capsulatus* cytochrome c_2. To assess $F_{CO\rightarrow H}$, the pulse sequence of Fig. 1 is simply started after the NOE mixing, labelled as time point ❷ in the sequence. This allows a residue-specific measurement of $F_{CO\rightarrow H} \times CO_z^{eq}$, provided that one starts from a fully relaxed spin state. These values can be used to replace the $F_{CO\rightarrow H} \times C_z^{\alpha^{eq}}$ contribution to the measured NOE, as the equilibrium magnetizations of CO and C^α are the same.

The cross-relaxation rates σ_{COC^α} are derived by fitting the experimental buildup curve, normalized by the two scaling factors ($F_{H\rightarrow C^\alpha}$ and $F_{CO\rightarrow H} \times C_z^{\alpha^{eq}}$), with the theoretical expression given in Eq. 2, to which an additional term is added that takes into account a possible DC offset. After fitting, the latter term was found to be close to zero within the experimental noise range, showing that

the experiments are not biased by preexisting CO_z magnetization. This procedure, rather than a simple linear fit of a few data points sampled at short mixing times, yields a better precision of the results by extending the data points to mixing times with higher signal-to-noise ratios.

Typical examples of normalized buildup curves of $^{13}C^{\alpha} \rightarrow {}^{13}CO$ cross relaxation in *Rb. capsulatus* cytochrome c_2 are shown in Fig. 2. The negative sign of $\sigma_{COC^{\alpha}}$ has been deduced from the opposite phase of the cross peaks in the CONH calibration experiment with respect to the NOE experiments. Note that the spread of the data points over times $\tau_m < 1.2$ s only permits the accurate determination of $\sigma_{COC^{\alpha}}$, but not that of $\rho_{C^{\alpha}}$ and ρ_{CO}. Estimated error bars on the normalized intensities are indicated in Fig. 2.

In Fig. 3, the cross-relaxation rates $\sigma_{COC^{\alpha}}$ are reported as a function of the polypeptidic sequence of cytochrome c_2. By a statistical error analysis, one can estimate the relative errors on $\sigma_{COC^{\alpha}}$ from the S/N in the NOE and the calibration experiments and from the errors in the curve fit. The cross-relaxation rates of residues preceding a proline are missing for lack of an amide proton, as well as a few overlapping ^{1}H-^{15}N correlation peaks.

The overall correlation time of cytochrome c_2 according to the Stokes–Einstein model of a rigid sphere is $\tau_c \approx 6$ ns; it has been experimentally confirmed by ^{15}N relaxation measurements (M. Caffrey, personal communication). The cross-relaxation rate $\sigma_{COC^{\alpha}}$ is given by the Redfield theory:

$$\sigma_{COC^{\alpha}} = \frac{1}{10}\left(\frac{\mu_0}{4\pi}\right)^2\left(\frac{\gamma^2\hbar}{r^3_{C^{\alpha}CO}}\right)^2 \times \left\{6J(\omega_{CO}+\omega_{C^{\alpha}}) - J(\omega_{CO}-\omega_{C^{\alpha}})\right\} \quad (4)$$

Assuming isotropic tumbling of a rigid molecule in solution ($J(\omega) = \tau_c / \{1 + (\omega\tau_c)^2\}$), a theoretical value of $\sigma_{COC^{\alpha}} = -0.10$ s^{-1} can be computed with $r_{C^{\alpha}CO} = 1.52$ Å. Since only motions faster than the overall tumbling rate contribute to the relaxation, internal flexibility – characterized by $S^2 < 1$ in the Lipari–Szabo model – may *increase* $\sigma_{COC^{\alpha}}$ above -0.1 s^{-1} (i.e., decreases its absolute value), but cannot decrease it. In Fig. 3, it can be seen that a fraction of the residues is above -0.1 s^{-1}, as predicted by the theory, but that a fair number is below this value.

This surprising result has been analysed in detail. As discussed above, great care has been taken to avoid any direct excitation of the CO spin before τ_m. At $\tau_m = 0$, all peaks are smaller than 0.008 (normalized intensity defined in Fig. 2) and thus within the experimental noise. An underestimation of the $F_{CO\rightarrow H}$ CO_z coefficient would lead to an overestimation of $\sigma_{COC^{\alpha}}$: the reference experiment starting from CO_z has been sampled with a recycle delay of 8 s $\approx 5 \times T_1(CO)$. A transfer mechanism through transverse coherences during τ_m can also be excluded: creation of zero-quantum coherences requires a CO pulse before τ_m and other x-y coherence should be destroyed by field gradients. We have concluded above that the efficiency of transfer via CSA–dipole cross-relaxation is negligible. An ultimate explanation – a high sensitivity of anisotropic overall tumbling – would require a complete investigation of this feature, which is beyond the scope of this paper.

The precision of the data strongly varies from one residue to another, as a result of the large disparity in heteronuclear coherence transfer efficiencies. Therefore, in view of the experimental precision, small differences between neighbours (± 0.02) are not meaningful. Even if the offset observed on $\sigma_{COC^{\alpha}}$ between the theory and the experimental data is not clarified, the values shown in Fig. 3 can be analysed in a relative way.

All cytochromes (Moore and Pettigrew, 1990) (including *Rb. capsulatus* cytochrome c_2 (Gooley et al., 1990; Benning et al., 1991)) exhibit a quite stable helix at the C-terminus. A periodic pattern is observed for the C-terminal helix (residues 103 to 115): residues 105, 106, 110 and 113 display less internal flexibility than their nearest neighbours. The N-terminal helix, which interacts with the C-terminal one via aromatic residues, shows the same behavior, with motional restriction for residues 5 and 9.

Another interesting pattern is noteworthy: a significant amount of glycines (residues 24, 42, 64, 80, 103 ...) exhibit $\sigma_{COC^{\alpha}}$ values above -0.1 s^{-1}. Because we have compensated for the different behavior of glycine in the INEPT sequence, this is evidence of a small S^2 for these residues. This result is in agreement with the peculiar role of glycines in proteins, incorporated at positions where flexibility is necessary for the biological function.

In this communication, an experimental pulse scheme for the measurement of site-specific $^{13}C^{\alpha}$-^{13}CO cross-relaxation rates has been proposed. We have applied this technique to a 116-residue protein, *Rb. capsulatus* cytochrome c_2, and have interpreted the variation of cross-relaxation rates in terms of local mobility. As it samples the motional properties differently from ^{1}H-^{13}C or ^{1}H-^{15}N relaxation experiments, the technique looks promising for studying the dynamics of proteins over a wider range of frequencies. The slight discrepancies observed between these results and other data on cytochrome c_2 are currently under investigation in our laboratory. One explanation might be that the motion experienced by the C^{α}-CO vector is likely to have a different geometry, mode of reorientation and, consequently, order parameter than those of an NH vector.

Acknowledgements

We thank Drs Michael Caffrey, Martin J. Blackledge and Prof. Erik Zuiderweg for stimulating discussions and Prof. M.A. Cusanovich for the preparation of the doubly labelled cytochrome c_2. This is publication #330 of the Institut de Biologie Structurale.

References

Bax, A., Mehlkopf, A.F. and Smidt, J. (1979) *J. Magn. Reson.*, **35**, 167–169.

Benning, M.M., Wesenberg, G., Caffrey, M.S., Bartsch, R.G., Meyer, T.E., Cusanovich, M.A., Rayment, I. and Holden, H.M. (1991) *J. Mol. Biol.*, **220**, 673–685.

Brooks III, C.L., Karplus, M. and Pettitt, B.M. (1988) *Adv. Chem. Phys.*, **71**, 1–249.

Chandrasekhar, I., Clore, G.M., Szabo, A., Gronenborn, A.M. and Brooks, B.R. (1992) *J. Mol. Biol.*, **226**, 239–250.

Engelke, J. and Rüterjans, H. (1995) *J. Biomol. NMR*, **5**, 173–182.

Goldman, M. (1984) *J. Magn. Reson.*, **60**, 437–452.

Gooley, P.R., Caffrey, M.S., Cusanovich, M.A. and MacKenzie, N.E. (1990) *Biochemistry*, **29**, 2278–2290.

Grzesiek, S. and Bax, A. (1992) *J. Magn. Reson.*, **96**, 432–440.

Ikuta, S. and Wang, Y.-S. (1990) *J. Am. Chem. Soc.*, **112**, 5901–5906.

Kay, L.E., Torchia, D.A. and Bax, A. (1989) *Biochemistry*, **28**, 8972–8979.

Kopple, K.D., Wang, Y.-S., Cheng, A.G. and Bhandary, K.K. (1988) *J. Am. Chem. Soc.*, **110**, 4168–4176.

Lipari, G. and Szabo, A. (1982a) *J. Am. Chem. Soc.*, **104**, 4546–4559.

Lipari, G. and Szabo, A. (1982b) *J. Am. Chem. Soc.*, **104**, 4559–4570.

Marion, D., Ikura, M., Tschudin, R. and Bax, A. (1989) *J. Magn. Reson.*, **85**, 393–399.

Moore, G.R. and Pettigrew, G.W. (1990) *Cytochromes c: Evolutionary, Structural and Physiological Aspects*, Springer, Berlin.

Peng, J.W. and Wagner, G. (1992a) *Biochemistry*, **31**, 8571–8586.

Peng, J.W. and Wagner, G. (1992b) *J. Magn. Reson.*, **98**, 308–332.

Smith, L.J., Mark, A.E., Dobson, C.M. and Van Gunsteren, W.F. (1995) *Biochemistry*, **34**, 10918–10931.

Sørensen, O.W. and Ernst, R.R. (1983) *J. Magn. Reson.*, **51**, 477–489.

Van Gunsteren, W.F. (1993) In *Computer Simulation of Biomolecular Systems: Theoretical and Experimental Applications*, Vol. 2 (Eds, Van Gunsteren, W.F., Weiner, P.K. and Wilkinson, A.J.), ESCOM, Leiden, pp. 3–36.

Wagner, G. and Wüthrich, K. (1979) *J. Magn. Reson.*, **33**, 675–679.

Werbelow, L.G. and Grant, D.M. (1977) *Adv. Magn. Reson.*, **9**, 190–298.

Yamazaki, T., Muhandiram, R. and Kay, L.E. (1994) *J. Am. Chem. Soc.*, **116**, 8266–8278.

Zeng, L., Fischer, M.W.F. and Zuiderweg, E.R.P. (1996) *J. Biomol. NMR*, **7**, 157–162.

Zhu, G. and Bax, A. (1990) *J. Magn. Reson.*, **90**, 405–410.